Available online at www.sciencedirect.com
SCIENCE DIRECT
Thin Solid Films 477 (2005) 73–80
thin solid films
www.elsevier.com/locate/tsf

New soluble poly(2,3-diphenylphenylene vinylene) derivatives for light-emitting diodes

Sheng-Hsiung Yang, Jiun-Tai Chen, An-Kuo Li, Chun-Hao Huang, Kuei-Bai Chen, Bing-R. Hsieh, Chain-Shu Hsu*

Department of Applied Chemistry, National Chiao Tung University, Hsinchu 300, Taiwan

Abstract

Soluble poly(2,3-diphenylphenylene vinylene) (DP-PPV) derivatives, poly(2,3-diphenyl-5-(4-heptyloxy-4'-oxytrimethylenediphenyl)-phenylene vinylene) (**P1**), poly(2,3-diphenyl-5-[4-(4-pentylcyclohexyl)phenoxy]-propyl-*p*-phenylene vinylene) (**P2**) and poly(2,3-diphenyl-5-(2-(1, 4, 5-triphenyl-1*H*-2-imidazoloyl)-1-oxytrimethylene phenyl) phenylene vinylene) (**P3**), were synthesized. **P1** and **P2** contain liquid crystal side groups; while **P3** contains a charge transport group. The polymers showed solid state UV–Visible absorption and photoluminescence in the range of 370–380 and 480–510 nm, corresponding to blue green emission. Similar to many other reported systems, the solution fluorescence spectra of **P1** and **P2** showed slight solvent dependency and blue-shifted with respect to those of the films. These were not the case for **P3** which showed little solvent dependency and little blue shift in solution. Two-layer light-emitting devices with a simple ITO/PEDOT/polymer/Ca (Al) configuration were fabricated and characterized.

Keywords: Conjugated polymer; Poly(2,3-diphenylphenylene vinylene); Electroluminescent devices

1. Introduction

Polymers based on poly(phenylene vinylene) and poly(dialkylfluorenes) show great promise for organic light-emitting diode (OLED) application [1–5]. We have been interested in poly(2,3-diphenylphenylene vinylene) (DP-PPV) derivatives, such as DP-PPV, DP6-, DP8-, and DP10-PPV shown below for the same application [6,7]. It has also been reported that DP-PPV derivatives (shown below) showed promising properties for organic laser application [8]. The advantages of this family of materials include (1) high glass transition temperatures, (2) high fluorescence efficiency (65–85%), (3) ease of monomer and polymer syntheses, and (4) broad molecular design latitudes [9].

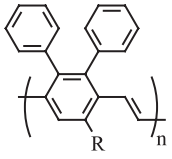

DP-PPV, R = H
DP6-PPV, R = C_6H_{13}
DP8-PPV, R = C_8H_{17}
DP10-PPV, R = $C_{10}H_{21}$

The key synthetic step that enables the broad molecular design latitude is the Diels–Alder reaction shown below, wherein Ar is an aromatic group, PG and PG′ are polymerizable groups, and R and R′ are aliphatic or aromatic groups. Since there are numerous Ar, R and R′ groups as well as many PG groups and PG′ groups, numerous monomers can be prepared similarly. These monomers can be used for the synthesis of both conjugated and non-conjugated functional aromatic polymers via condensation or coupling polymerization. One design strategy is to select a long-chain aliphatic group for R and/or R′ to

* Corresponding author.
E-mail address: cshsu@mail.nctu.edu.tw (C.-S. Hsu).

0040-6090/$ - see front matter © 2004 Elsevier B.V. All rights reserved.
doi:10.1016/j.tsf.2004.08.113

prevent insolubility problem generally associated with aromatic polymers, especially for conjugated polymers. Of course one can also incorporate solubilizing groups on Ar.

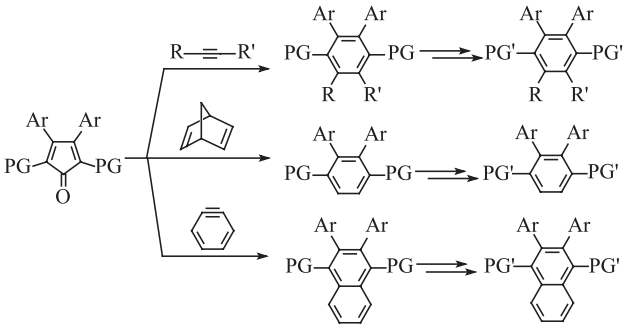

PG = -COOEt, -CH_3, -$COCH_3$, -Ph, -Ph-Br, -Ph-COOEt, -Ph-NO_2 etc.
PG'= -CHO, -$COCH_3$, -$COCH_2Ph$, -COOH, -COCl, -CH_2Cl, -CH_2CN, Ph-NH_2, Ph-CH_2Cl etc

We have reported the synthesis of several DP-PPV derivatives [10]. Here we report the synthesis of three new DP-PPV derivatives (poly(2,3-diphenyl-5-(4-heptyloxy-4'-oxytrimethylenediphenyl)phenylene vinylene) (**P1**), poly(2,3-diphenyl-5-[4-(4-pentylcyclohexyl)phenoxy]-propyl-*p*-phenylene vinylene) (**P2**) and poly(2,3-diphenyl-5-(2-(1, 4, 5-triphenyl-1*H*-2-imidazoloyl)-1-oxytrimethylene phenyl) phenylene vinylene) (**P3**) see Scheme 2), their light emission properties, and other relevant physical properties. **P1** and **P2** contain liquid crystal side groups; while **P3** contains a charge transport group.

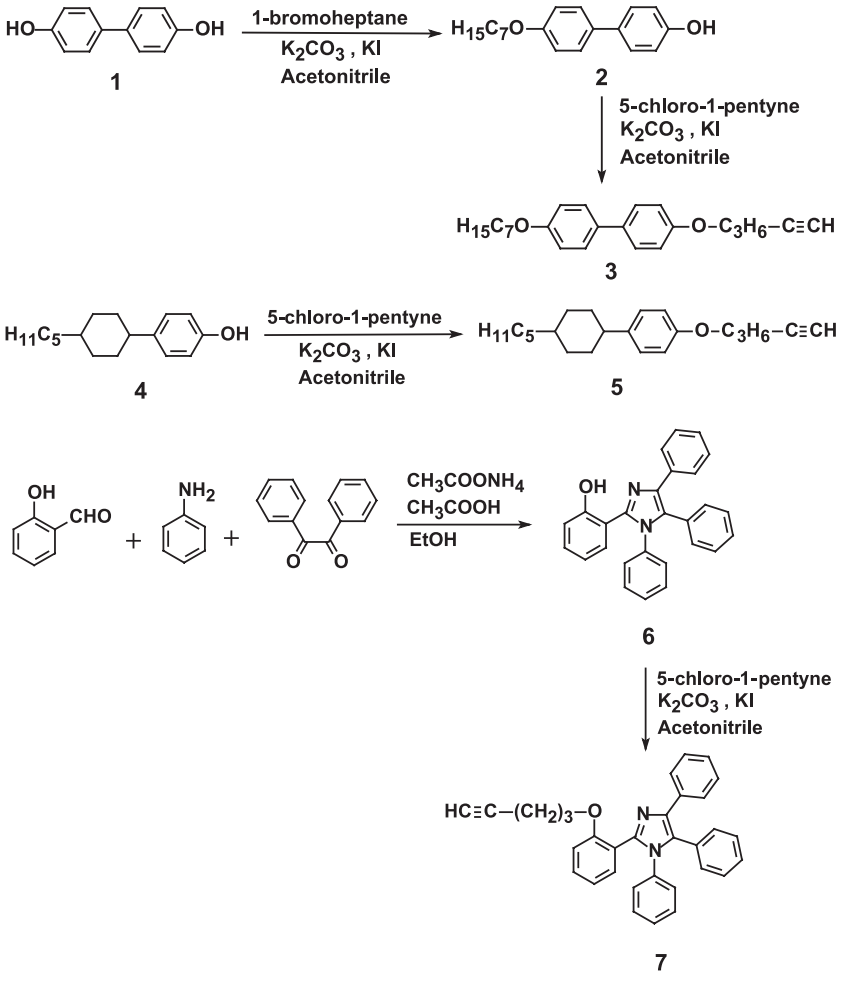

Scheme 1. Synthesis of functional acetylene compounds **3**, **5**, and **7**.

2. Synthesis and characterization of P1–P3

The synthetic sequences of **P1**, **P2** and **P3** are shown in Schemes 1 and 2. Scheme 1 shows the synthesis of functional acetylene compounds **3**, **5** and **7**. 4,4′ -Biphenol (**1**) is monoalkylated to give **2** which is alkylated with 5-chloro-1-pentyne to give **3**. Similar alkylation of **4** gives **5**. Compound **6**, which was prepared from condensation of salicyladehyde, benzil and aniline under acidic condition, is also similarly alkylated to give **7**. As shown in Scheme 2, **3**, **5**, and **7** undergo Diels-Alder reaction with 2,5-Bis(ethoxycarbonyl)-3,4-diphenylcyclopentadienone (**8**) to give **9a-c**, respectively. In order to improve the reactivity of Diels–Alder reaction of **3**, **5** and **7** with cyclopentadienone, the reaction uses solvent-free condition and melts the mixture under 120 °C stirring for 12 h.

These are reduced with $LiAlH_4$ to give the respective **10a–c** which then react with thionyl chloride to give monomers **11a–c**. Normally, the reduction of diesters with $LiAlH_4$ can be accomplished with stirring at room temperature for several hours as was found for the reduction of 2,5-diphenylterphthalate. However, the sterically hindered diesters (**9a–c**) had to be refluxed overnight to reduce both ester groups to the alcohol. All substituted DP monomers were identified by NMR and elemental analysis. Polymerization of **11a**, **11b**, and **11c** in the presence of large excess of potassium *tert*-butoxide (*t*-BuOK) gives **P1**, **P2** and **P3**, respectively.

In order to find out the amount of base needed to eliminate HCl completely, we experimented with 8, 12, and 16 equivalents of *t*-BuOK. From ^{1}H-NMR spectra, we found that polymers prepared from 8 and 12 equivalents of base still gave peaks at 4.3–4.4 ppm, which can readily be assigned to the proton signal for –CHCl. These polymers also showed weight loss during TGA measurement at about 190 °C, which is the typical cleavage temperature of C–Cl bond. With 16 equivalents of base, we were able to obtain polymers free from the –CHCl peak and without weight loss. All the results above show that 16 equiv of *t*-BuOK is the best amount used to carry out polymerization. No gelation is observed during polymerization. The polymers were isolated by precipitation in MeOH, followed by purification by redissolving in $CHCl_3$ and precipitating into methanol three times. The polymers were then dialyzed successively in acetone, water and methanol for 2 days each. The polymers were highly soluble in common organic solvents such as THF, chloroform, dichloromethane, and toluene. All polymers possess high molecular weights and narrow molecular weight distribution. The weight-average molecular weight (Mw) and polydispersity (PD) for polymers **P1**, **P2** and

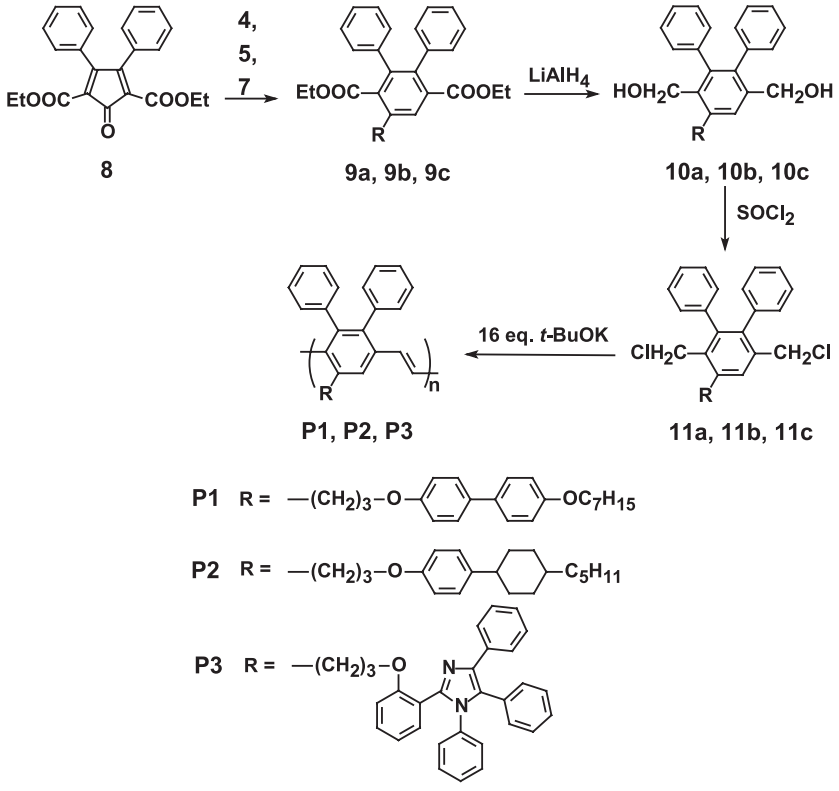

Scheme 2. Synthesis of polymers **P1**–**P3**.

Table 1
Optical properties of the polymers

Polymer	Absorption				Fluorescence			
	In THF λ_{max} (nm)	In $CHCl_3$ λ_{max} (nm)	In toluene λ_{max} (nm)	Films λ_{max} (nm)	In THF λ_{max} (nm)	In $CHCl_3$ λ_{max} (nm)	In toluene λ_{max} (nm)	Films λ_{max} (nm)
P1	348	339	378	381	473	475	502	503
P2	NA[a]	357	NA[a]	381	NA[a]	476	NA[a]	494
P3	358	360	358	375	477	477	474	483
PPV	NA[b]	NA[b]	NA[b]	440	NA[b]	NA[b]	NA[b]	565
DP-PPV	NA[b]	NA[b]	NA[b]	405	NA[b]	NA[b]	NA[b]	505

[a] Slight soluble in THF and toluene.
[b] Insoluble in organic solvents.

P3 are 226 K, 1.53, 401 K, 1.97 and 418 K, 2.91, respectively.

3. Mesomorphic behaviors

The thermotropic liquid crystalline phase of **P1** and **P2** was investigated by differential scanning calorimetry (DSC) and a polarized optical microscope (POM). The glass transition temperature (T_g) of **P1** and **P2** are 172 and 156 °C, respectively. An apparent endothermic peak at 290 °C is assigned to the melting point (T_m) of **P1** and we cannot see it of **P2** up to 300 °C in DSC diagram. Typical nematic textures of the polymers are shown in Fig. 1. A stable mesophase with a threaded texture and large domains was observed for **P1** at 200 °C. Similarly, a mesophase with a very fine treaded texture was observed for **P2** at 190 °C. The optical texture of the sample was almost unchanged after it was quenched to room temperature. This is advantageous for our further application in rubbing alignment process.

4. Optical properties

Absorption and emission spectra were measured in THF, $CHCl_3$, Toluene, and in the solid state. Fig. 2 shows the UV–Vis absorption and fluorescence spectra of these polymers as solid film and in THF. The wavelengths of absorption and emission maxima are listed in Table 1. The film of **P1** has an absorption maximum (λ_{max}) at 381 nm, which is about 70 and 35 nm blue-shifted as compared to PPV and DP-PPV, respectively. This can be attributed to the bulky substituents of the two phenyl rings and the pendant alkyl groups that interrupt the planarity of the main chain and thus reduce the degree of conjugation. The λ_{max} of **P1** at 339 nm in chloroform, 348 nm in THF, and 378 nm in toluene, is blue-shifted with respect to that of the film. Similar results were obtained for **P2** and **P3**. The absorption maxima of the films are slightly red-shifted as compared to those in solutions, consistent with other poly(*p*-phenylene vinylene)-related polymers [11].

The new DP-PPV polymers are highly fluorescent in the solid state as well as in dilute solution. As shown in Fig. 2 and Table 1, PL spectra of **P1** and **P2** in low polarity solvent, such as toluene and in the solid state are red-shifted with respect to those in polar solvents, suggesting that polymer aggregation is relatively strong in the non-polar solvents and solid state. Comparing with other PPVs such as MEH-PPV and polyfluorene where large PL peak wavelength difference of 40–60 nm between solid state and dilute solution was reported [8,12–14,17], we have the same PL wavelength-shifted tendency, but red-shifts are much

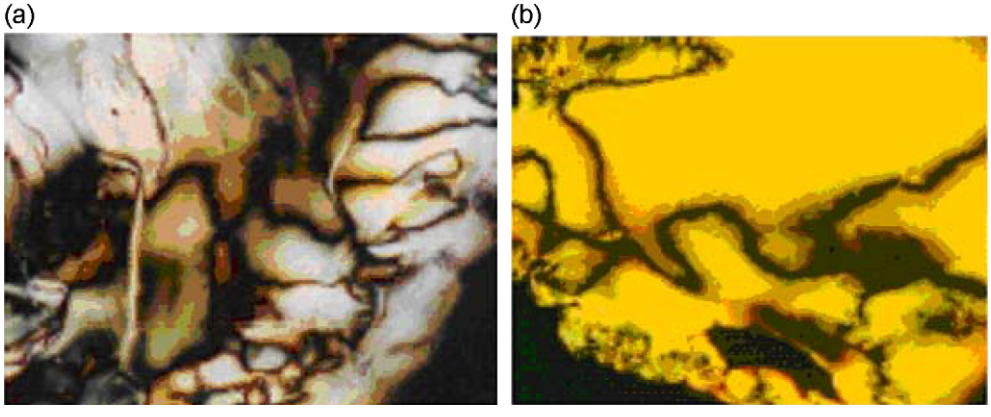

Fig. 1. Optical textures of (a) polymer **P1** at 200 °C and (b) polymer **P2** at 190 °C.

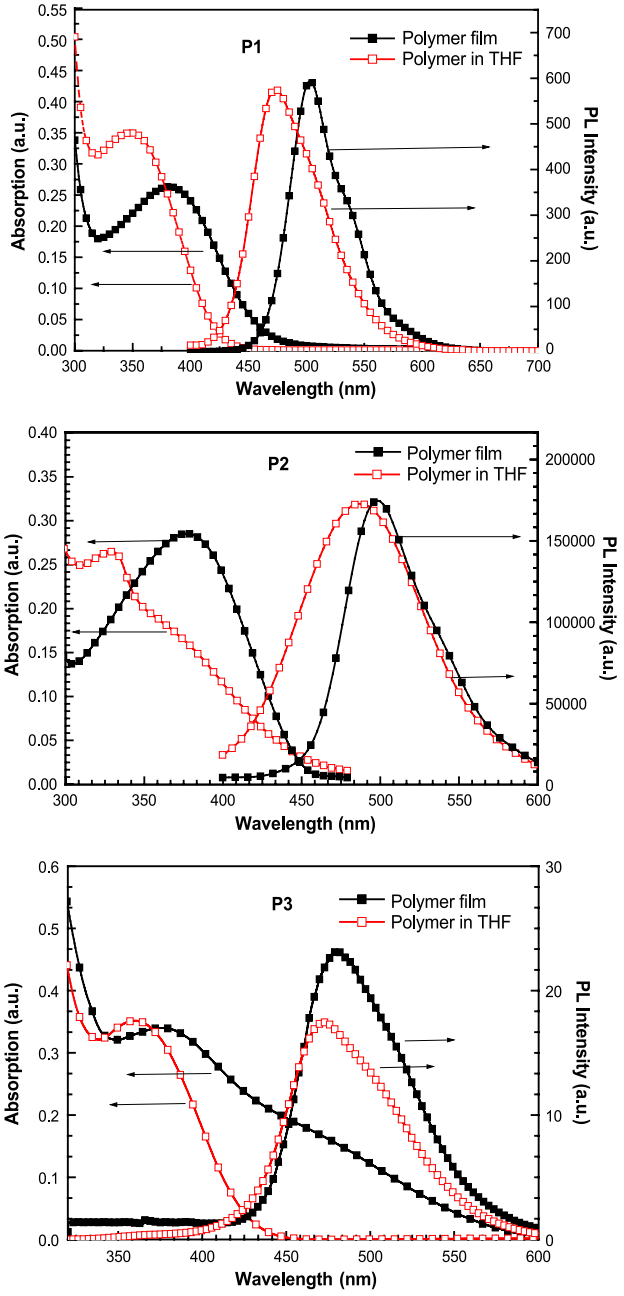

Fig. 2. UV–Vis and PL spectra of all polymers in solid state (solid square) and in THF solution (open square).

smaller for the DP-PPVs. This is most apparent for **P3**, its emission peak remains relatively unchanged in the solid state and in solutions. The fluorescence quantum yields (Φ_{fl}) of the polymers in THF were estimated by comparing with the standard of quinine sulfate (ca. 1×10^{-5} M solution in 0.1 M H_2SO_4, having a fluorescence quantum yield of 55%). The Φ_{fl} of **P1**, **P2** and **P3** are 0.57, 0.53 and 0.65, respectively. The results demonstrate that high PL yield polymers can be achieved by the introduction of the bulky side groups, since separation of the polymer backbones partially can prevent interchain exciton transfer. [12,15].

5. Polarized photoluminescent

We aligned **P1** and **P2** by a rubbing treatment at the LC state to give polarized optical properties. The UV dichroism measurement was performed in the presence of a polarizer inserted in parallel or in perpendicular (with respect to the rubbing direction) between the sample and the light source. As shown in Fig. 3, a significantly larger absorption ascribed to a π–π* transition can be seen at the perpendicular polarized direction for **P1**. Rubbing-induced chain alignment of **P1** was also detected by a polarized PL measurement. The dichroic PL spectra of **P1** are also shown in Fig. 3, indicating that the light emitted from the rubbed film was preferentially polarized perpendicular to the rubbing direction. This is because rubbing at thermotropic liquid crystalline phase induces alignment of the LC side groups along the rubbing direction and the alignment of the polymer backbones perpendicular to the rubbing direction (Fig. 4). As a result, relatively large absorption and emission are observed in the orthogonal direction with respect to the rubbing direction. The dichroic ratio, defined as the perpendicular to parallel fluorescence intensity, was 2.1 which was better than dialkoxy side chain liquid crystalline PPVs and PTVs (1.2–1.4) [16]. However, we did not see large difference in peak intensity between rubbed and unrubbed films. This suggests that alignment may occur only at the top surface and not in the bulk film.

6. Electrochemical study

The cyclic voltammograms of compound **6** and **P1**–**P3** (Fig. 5) absorbed on a Pt wire from toluene solution were performed in an electrochemical cell with a Pt counter electrode and a Hg reference electrode. From the different onset potentials, and the band gaps calculated from the onsets of UV absorption, the band diagrams were determined [17,18] and displayed in Fig. 6. It can be

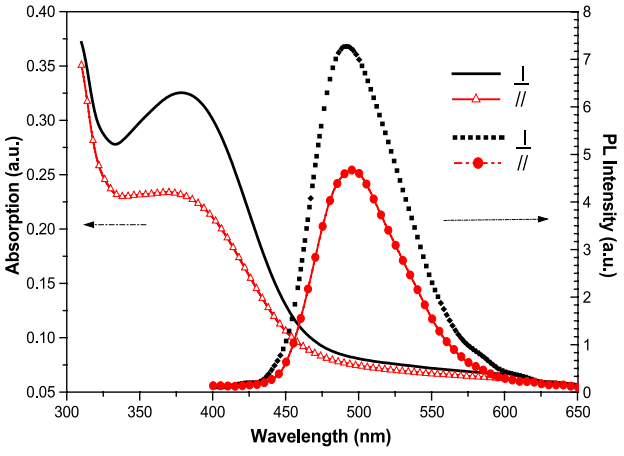

Fig. 3. Polarized optical absorption spectra and PL spectra of polymer **P1**.

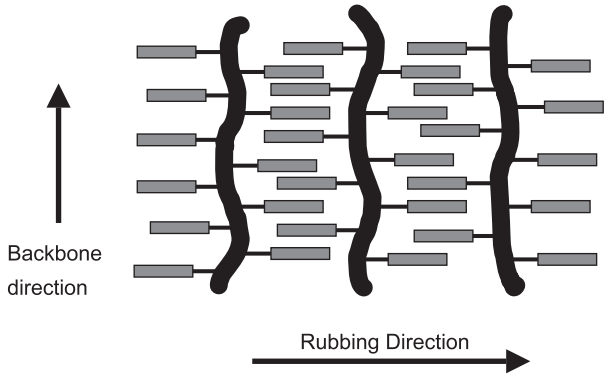

Fig. 4. Alignment of LC side groups and polymer backbones due to rubbing treatment.

seen that all DP polymers show similar HOMO-LUMO levels suggesting that the pendant groups do not change the electronic state of the polymer significantly, although they may help the charge transport and injection. This resembles the molecularly doped system. The cyclic voltagram of **6** shown in the inset of Fig. 5c suggests that it is a one-electron transport material that can be easily reduced. The oxidation potential for imidazole is 0.52 V, corresponding to a HOMO level of 4.92 eV. This suggests that removal of electrons from **6** to ITO can readily occur. However, the effect of the imidazole group cannot readily be seen from Fig. 6.

7. Electroluminescence

Double-layer LED devices ITO/PEDOT:PSS/Polymer/Ca(Al) were fabricated by spin coating the polymer solution onto ITO-coated glass substrates. The coating thickness of PEDOT and polymers was about 1000 Å, and the active areas were 0.09 cm^2. The EL spectra of the polymers are shown in Fig. 7. All polymers showed bluish-green emission at around 490 nm, in good agreement with the PL emission peaks. These results suggest that EL and PL come from similar excited states. The current–voltage–luminance characteristics of three polymers are shown in Fig. 8. The turn-on voltage of the **P1** device is 11 V with a maximum brightness of 420 cd/m^2 and maximum EL yield of 0.79 cd/A at 16 V. The turn-on voltage of the **P2** device is 10 V with a maximum brightness of 70 cd/m^2 and maximum EL yield of 0.33 cd/A at 24 V. The turn-on voltage of the **P3** device is 8 V with a maximum brightness of 22 cd/m^2 and maximum EL yield of 0.11 cd/A at 12 V. The lower turn-on voltage of **P3** may be due to the introduction of imidazole charge transport side group, which results in an increase of charge transport properties. However, the three polymers still did not show reduced driving voltage as compared with the unsubstituted DP-PPV. This suggests that the DP-PPV polymer backbone controls the fundamental electro-optical properties of this series polymer. Although the present polymers have high PL quantum efficiency, they did not show high electroluminescent as other substituted PPV polymers such as MEH-PPV did.

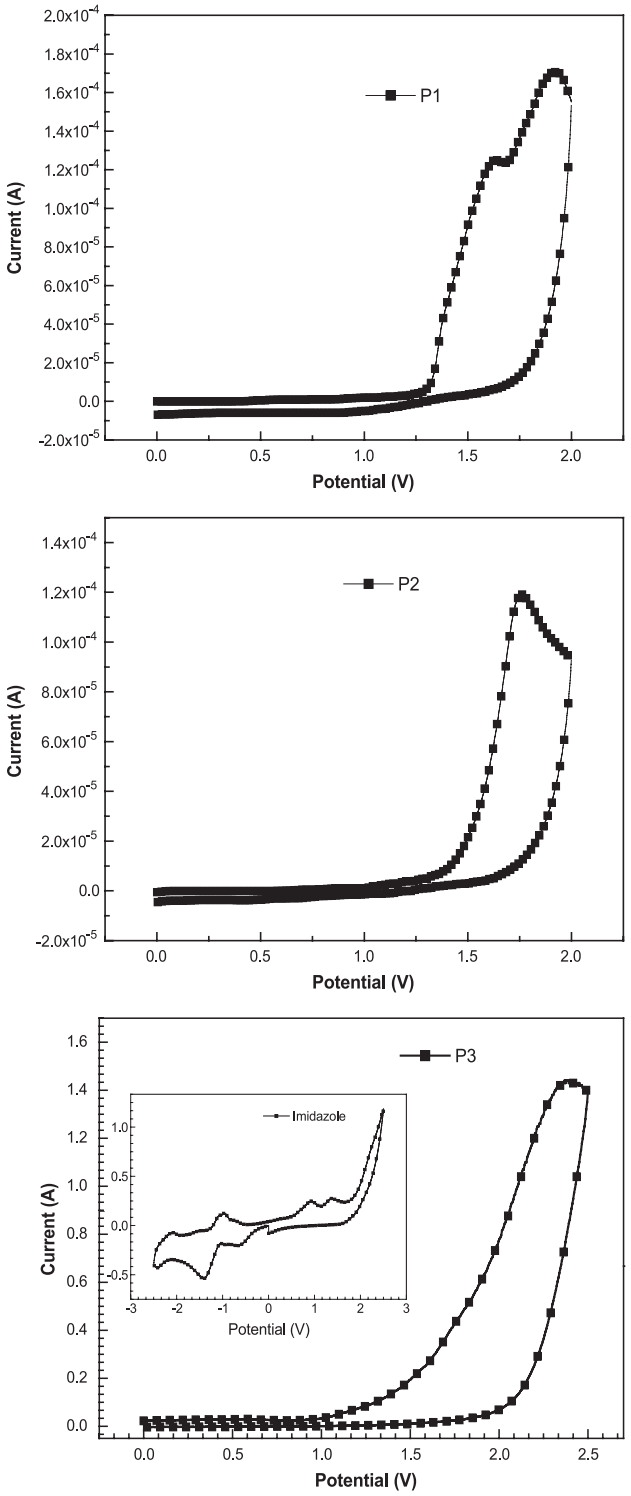

Fig. 5. Cyclic voltammograms of polymer films dip-coated on platinum plate electrodes in acetontrile containing 0.1 M Bu_4NBF_4. Platinum wire as the counter electrode. The potentials reference against Ag/0.1M $AgNO_3$ in acetonitrile. Scan rate: 50 mV/s.

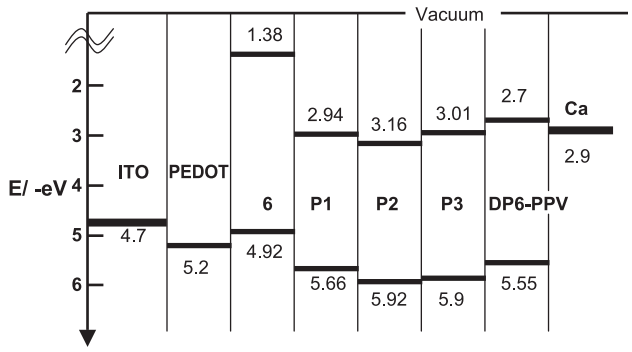

Fig. 6. Band diagram of **6**, DP6-PPV, **P1**, **P2**, and **P3** used in this study. The position of the valence band (HOMO) is estimated from electrochemical studies, and the band gap (HOMO-LUMO) from the onset of optical absorption.

This may be attributable to the very order packing of DP-PPV backbones which was proved by X-ray diffractions [19].

8. Summary

We synthesized three substituted DP-PPV derivatives, and the PL and EL properties were characterized. The three bulky substituents make the polymer chain rotation, forming *cis*-and *trans*-structures, and non-aggregation. The three things make our polymers show blue shift and high PL efficiency with respect to the traditional PPV. An improvement of the emission properties compared with traditional DP-PPVs was obtained from the three polymers as the double layer devices of the type ITO/PEDOT:PSS/Polymer/Ca(Al). Device fabricated by **P1** turn on at 11 V and a maximum luminance of 433 cd/m^2 could be observed at 17 V applied voltage. This is the brightest DP-PPV EL device so far. We

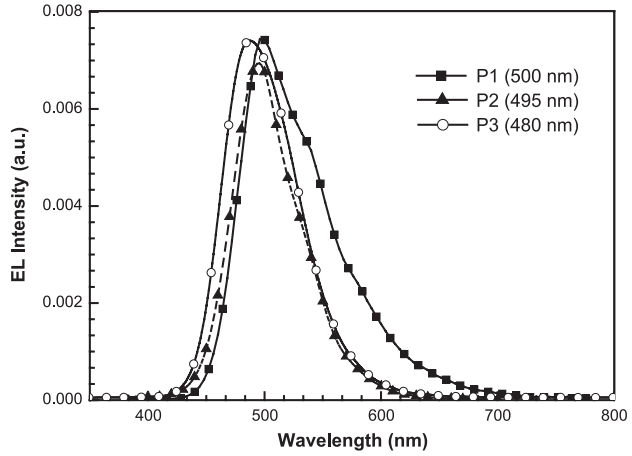

Fig. 7. Electroluminescence spectra of the polymers **P1** (■), **P2** (▲), and **P3** (○).

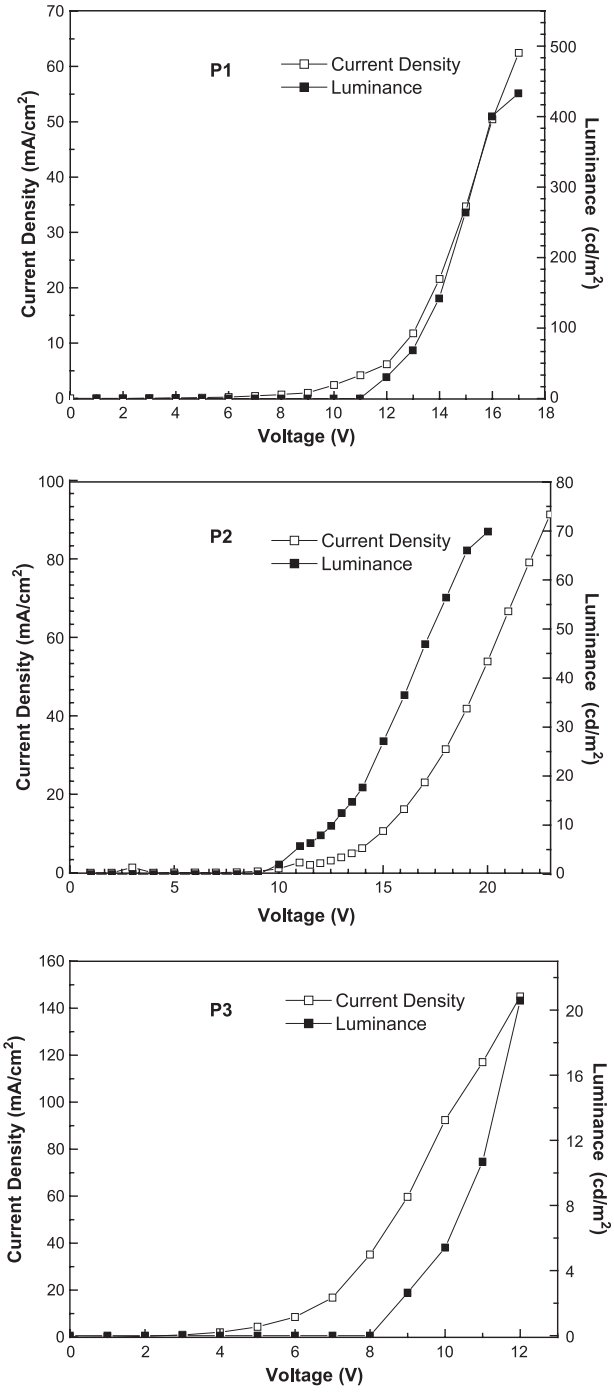

Fig. 8. Current–voltage–luminescence characteristics of ITO/PEDOT/polymers/Ca(Al).

also showed clear evidence of nematic LC phases in the polymers **P1** and **P2**. The polymers can be aligned by traditional rubbing treatment to give linearly dichroic PL with a dichroic ratio of 2.1. The decrease of the driving voltage of **P3** is due to the introduction of imidazole group to decrease the band offset between polymer and hole injection electrode. In this result, we successfully could obtain a low driving voltage electroluminescent

DP-PPV polymer by adopting the charge transport side group.

Acknowledgements

The authors are grateful to the National Science Council of the Republic of China (NSC90-2216-E-009-019) for its financial support of this work.

References

[1] (a) J.H. Burroughes, D.D.C. Bradley, A.R. Brown, R.N. Marks, K. Mackay, R.H. Friend, P.L. Burn, A.B. Holms, Nature 347 (1990) 539;
(b) D. Braun, A.J. Heeger, Appl. Phys. Lett. 58 (1991) 1982;
(c) H. Spreitzer, H. Becker, E. Kluge, W. Kreuder, H. Schenk, R. Demandt, H. Schoo, Adv. Mater. 10 (1998) 1340.
[2] A.R. Brown, N.C. Greenham, J.H. Burroughes, D.D.C. Bradley, R.H. Friend, P.L. Burn, A. Kraft, A.B. Holmes, Chem. Phys. Lett. 200 (1992) 46.
[3] H. Spreitzer, H. Becker, E. Kluge, W. Kreuder, H. Schenk, R. Demandt, H. Schoo, Adv. Mater. 10 (1998) 1340.
[4] M.T. Bernius, M. Inbasekaran, J. O'Brien, W. Wu, Adv. Mater. 12 (2000) 1737.
[5] I.S. Millard, Synth. Met. 111–112 (2000) 119.
[6] B.R. Hsieh, Y. Yu, E.W. Forsythe, G.M. Schaaf, W.A. Feld, J. Am. Chem. Soc. 120 (1998) 231.
[7] (a) W.C. Wan, H. Antoniadis, V.E. Choong, H. Razafitrimo, Y. Gao, W.A. Feld, B.R. Hsieh, Macromolecules 30 (1997) 6567;
(b) H. Antoniadis, D. Roitman, B.R. Hsieh, W.A. Feld, Polym. Adv. Technol. 8 (1997) 392.
[8] M.D. McGehee, A.J. Heeger, Adv. Mater. 12 (2000) 1655.
[9] B.R. Hsieh, Y.Yu, U.S. Patent 5,945, (1999), 502.
[10] (a) B.R. Hsieh, W.C. Wan, Y. Yu, Y. Gao, T.E. Goodwin, S.A. Gonzalez, W.A. Feld, Macromolecules 31 (1998) 631;
(b) A.K. Li, S.S. Yang, W.Y. Jean, C.S. Hsu, B.R. Hsieh, Chem. Mater. 12 (2000) 2741.
[11] D.M. Johansson, X. Wang, T. Johansson, O. Inganas, G. Yu, G. Srdanov, M.R. Andersson, Macromolecules 35 (2002) 4997.
[12] (a) Y. Shi, J. Liu, Y. Yang, J. Appl. Phys. 87 (9) (2000) 4254;
(b) Y. Shi, J. Liu, Y. Yang, Macromol. Symp. 154 (2000) 187.
[13] B. Liu, W.L. Yu, Y.H. Lai, W. Huang, Chem. Mater. 13 (2001) 1984.
[14] C. Xia, R.C. Advincula, Macromolecules 34 (2001) 6922.
[15] D.K. Fu, B. Xu, T.M. Swager, Tetrahedron 53 (44) (1997) 15487.
[16] (a) H. Goto, K. Akagi, H. Shirakawa, S.H. OH, K. Araya, Synth. Met. 71 (1995) 1899;
(b) K. Akagi, J. Oguma, S. Shibata, R. Toyoshima, I. Osaka, H. Shirakawa, Synth. Met. 102 (1999) 1287;
(c) J. Oguma, K. Akagi, H. Shirakawa, Synth. Met. 101 (1999) 86.
[17] N.H.S. Lee, Z.K. Chen, S.J. Chua, Y.H. Lai, W. Huang, Thin Solid Films 363 (2000) 106.
[18] Z.K. Chen, W. Huang, L.H. Wang, E.T. Kang, B.J. Chen, C.S. Lee, S.T. Lee, Macromolecules 33 (2000) 9015.
[19] I.F. Huang, PhD thesis, Institute of Material Science and Engineering, National Sun Yat-sen University, Taiwan, 2002.

Further reading

(a) B.A. Reinhardt, Carboethoxy-Substituted Polyphenylenes MS Thesis, WSU, 1971;
(b) W.H. Harris, B.A. Reinhardt, Polym. Prepr. (Am. Chem. Soc., Div. Polym. Chem.) 15 (1) (1974) 691;
(c) W.C. Wan, H. Antoniadis, V.E. Choong, H. Razafitrimo, Y. Gao, W.A. Feld, B.R. Hsieh, Macromolecules 30 (1997) 6567.